

Environmental mobility of ^{110m}Ag: lessons learnt from Fukushima accident (Japan) and potential use for tracking the dispersion of contamination within coastal catchments

Hugo Lepage, O. Evrard, Yuichi Onda, Jérémy Patin, Caroline Chartin, Irène Lefevre, Philippe Bonté, Sophie Ayrault

▶ **To cite this version:**

Hugo Lepage, O. Evrard, Yuichi Onda, Jérémy Patin, Caroline Chartin, et al.. Environmental mobility of ^{110m}Ag: lessons learnt from Fukushima accident (Japan) and potential use for tracking the dispersion of contamination within coastal catchments. Journal of Environmental Radioactivity, 2014, 130, pp.44-55. 10.1016/j.jenvrad.2013.12.011 . cea-02614715

HAL Id: cea-02614715
https://cea.hal.science/cea-02614715

Submitted on 25 May 2020

HAL is a multi-disciplinary open access archive for the deposit and dissemination of scientific research documents, whether they are published or not. The documents may come from teaching and research institutions in France or abroad, or from public or private research centers.

L'archive ouverte pluridisciplinaire **HAL**, est destinée au dépôt et à la diffusion de documents scientifiques de niveau recherche, publiés ou non, émanant des établissements d'enseignement et de recherche français ou étrangers, des laboratoires publics ou privés.

Environmental mobility of ^{110m}Ag: lessons learnt from Fukushima accident (Japan) and potential use for tracking the dispersion of contamination within coastal catchments

Hugo Lepage[a,*], Olivier Evrard[a], Yuichi Onda[b], Jeremy Patin[b], Caroline Chartin[a], Irène Lefèvre[a], Philippe Bonté[a], Sophie Ayrault[a]

[a] Laboratoire des Sciences du Climat et de l'Environnement (LSCE/IPSL), Unité Mixte de Recherche 8212 (CEA, CNRS, UVSQ), 91198, Gif-sur-Yvette Cedex, France

[b] Center for Research in Isotopes and Environmental Dynamics (CRIED), University of Tsukuba, 1-1-1 Tennodai, Tsukuba, Ibaraki 305-8572, Japan

* Corresponding author.

E-mail address: hugo.lepage@lsce.ipsl.fr (H. Lepage).

Telephone: +33/1/69.82.43.33

Environmental mobility of ^{110m}Ag: lessons learnt from Fukushima accident (Japan) and potential use for tracking the dispersion of contamination within coastal catchments

Abstract

Silver-110 metastable (^{110m}Ag) has been far less investigated than other anthropogenic radionuclides, although it has the potential to accumulate in plants and animal tissues. It is continuously produced by nuclear power plants in normal conditions, but emitted in much larger quantities in accidental conditions facilitating its detection, which allows the investigation of its behaviour in the environment. We analysed ^{110m}Ag in soil and river drape sediment (i.e., mud drapes deposited on channel-bed sand) collected within coastal catchments contaminated in Fukushima Prefecture (Japan) after the Fukushima Dai-ichi Nuclear Power Plant accident that occurred on 11 March 2011. Several field experiments were conducted to document radiosilver behaviour in the terrestrial environment, with a systematic comparison to the more documented radiocesium behaviour. Results show a similar and low mobility for both elements in soils and a strong affinity with the clay fraction. Measurements conducted on sediment sequences accumulated in reservoirs tend to confirm a comparable migration and deposition of those radionuclides even after their redistribution due to erosion and deposition processes. Therefore, as the ^{110m}Ag:^{137}Cs initial activity ratio varied in soils across the area, we justified the relevance of using this tool to track the dispersion of contaminated sediment from the main inland radioactive pollution plume generated by FDNPP accident.

1. Introduction

Silver-110 metastable (^{110m}Ag) is a radioisotope with a rather short half-life of 249 days produced in nuclear power plants (NPP) as an activation product of ^{109}Ag. In NPP, natural silver (which contains 48% of ^{109}Ag) is found in control rods or in the alloy used to seal the head of the reactor (-Calmon and Garnier-Laplace 2002; Chelet 2006; IAEA 1998). In addition, ^{109}Ag may also be a fission product from uranium and plutonium (Chelet, 2006). ^{110m}Ag can be measured by spectrometry gamma (with the main peak at 658 keV, and secondary peaks at 885 and 937 keV).

Le Petit et al. (2012) described the ^{110m}Ag as a volatile fuel particle displaying some common characteristics with semi-volatile substances, due to its well-known strong retention within the reactor core structures. Even though ^{110m}Ag is produced by NPP in normal operational conditions, its release into the environment remains limited (Ciffroy et al., 2005; Eyrolle et al., 2012) (Table 1), and research on this radionuclide has mainly gained interest after Chernobyl and Fukushima Dai-ichi accidents when it was emitted in much larger quantities, which facilitated its measurement. A search of the Web of Knowledge citation index (July 2013) shows that the number of publications about ^{110m}Ag increased significantly after Chernobyl accident (Fig. 1). A similar increase in attention has already been observed shortly after Fukushima accident.

Few information are available on the environmental mobility of ^{110m}Ag, and most of the studies regarding this radioisotope were conducted in laboratory (Calmon and Garnier-Laplace 2002) because the conditions necessary to conduct field experiments were rarely met, as samples should be collected within the months following a release. They should alternatively be recovered in large quantities and analysed with high sensitivity detectors

during relatively long counting times. Still, it remains important to better understand its behaviour in the environment, as it has been demonstrated that silver is one of the most toxic metals (Bryan, 1971; Ratte, 1999) and that ^{110m}Ag may be transferred from the soils to the plants (Handl et al., 2000; Shang and Leung, 2003), and accumulated in animal tissues (Adam et al., 2001; Beresford et al., 1998; Bryan and Langston, 1992; Khangarot and Ray, 1987; Martin and Holdich, 1986; Oughton, 1989). It can also contaminate natural silver (isotopic contamination) used for photographic industry and jewellery manufacturing (Vuković, 2002).

Besides this interest to better understand the radioecology of ^{110m}Ag, it has been shown that this radioisotope was emitted by the Fukushima Dai-ichi Nuclear Power Plant (FDNPP) accident and subsequently detected in the environment (Fukuda et al., 2013; MEXT, 2011; Tazoe et al., 2012; Watanabe et al., 2012). It is estimated that 20% of the radionuclides emitted were deposited on the soils of Fukushima Prefecture as a result of wet and dry atmospheric fallout, creating a contamination plume extending up to 70 km to the northwest of the FDNPP site (Kinoshita et al., 2011; Yasunari et al., 2011). It was estimated that between 7 and 36 PBq of ^{137}Cs ($T_{1/2}$ = 30.17y) were released (Chino et al., 2011; Stohl et al., 2012; Winiarek et al., 2012), and ^{110m}Ag release rate represented about 11% of the ^{137}Cs rate (Petit et al., 2012).

Depending on the behaviour of the radionuclides and their affinity with the fine mineral particles and the associated organic matter fraction, they may subsequently be redistributed across hillslopes as a consequence of runoff and soil erosion processes and be delivered to downstream rivers that may finally supply them to the ocean (Tanaka et al., 2012; Tateda et al., 2013; Ueda et al., 2013). Even though the bulk of initial marine contamination originated

69 from atmospheric deposition, erosion processes may have partly supplied the ^{110m}Ag that
70 was detected in zooplankton in the Pacific Ocean shortly after the accident (Buesseler et al.,
71 2012).

72 In order to document this transfer, Chartin et al. (2013) showed that the spatial patterns of
73 ^{110m}Ag:^{137}Cs activity ratio in soils varied across space within the Fukushima contamination
74 plume. They subsequently used this ratio to track the dispersion of contaminated sediment
75 along a coastal river draining a catchment located within the main radioactive plume.

76 However, to date, most studies conducted in Fukushima post-accidental conditions focused
77 on ^{134}Cs and ^{137}Cs behaviour (Inoue et al. 2013; Koarashi et al. 2012; Kato et al. 2012a,
78 2012b; Matsunaga et al. 2013). Investigations reporting the presence of ^{110m}Ag in soil did not
79 detail its distribution with depth nor its behaviour (Fukuda et al., 2013; Tazoe et al., 2012;
80 Watanabe et al., 2012). In this context, there is a lack of data collected in this specific post-
81 accidental context to document the relative behaviour of ^{110m}Ag and ^{137}Cs in soils and
82 sediment in order to check the relevance of using this ratio to track the dispersion of
83 contaminated material along rivers. Even though both radionuclides are particle-reactive,
84 the ^{110m}Ag:^{137}Cs activity ratio in mobilized sediment might not simply reflect the catchment
85 soil average of this ratio.

86 In this context, this paper aims to compile original experimental data acquired in Fukushima
87 Prefecture during the months that followed the accident to document ^{110m}Ag behaviour in
88 soils and sediment. This paper will particularly address four issues:

89 (1) the affinity of ^{110m}Ag with different grain size fractions, to check whether there is a
90 different behaviour of ^{110m}Ag and ^{137}Cs depending on the particle size;
91 (2) the migration of ^{110m}Ag in the soil, to investigate its potential movement with depth;

(3) the evolution of ^{110m}Ag activities within sediment sequences accumulated in reservoirs, to document whether characteristics of contaminated sediments delivered to the reservoir by successive flood events change with time;

(4) the evolution of ^{110m}Ag activities within sediment drape deposits, that consist of mud drapes deposited on channel-bed sand (Olley et al., 2013), collected at the same locations along the rivers after a succession of typhoon and snowmelt events to investigate the impact of those events on ^{110m}Ag redistribution in catchments.

We will systematically compare the radiosilver behaviour to the one of the well documented radiocaesium, and to the literature data. The implications of those results will finally be discussed to decide whether the use of the ^{110m}Ag:^{137}Cs activity ratio is relevant to track the dispersion of contaminated sediment from the main radioactive pollution plume generated by FDNPP accident.

2. Materials and methods

2.1. Study area

The study was conducted in Fukushima Prefecture, located in Northeastern Japan. We focused on several coastal catchments (i.e. Mano, Nitta, Ota and Odaka catchments) (1000 km²) draining the main part of the radioactive plume extending to the northwest of FDNPP (Fig. 2). Those catchments extend from the coastal mountain range (at approximately 30-km distance of the coast) to the Pacific Ocean and their elevation ranges from 0 to 900 m.

Plateaus on the west consist of Cretaceous granite and granodiorite, evolving into a complex patchwork of volcanic (both intrusive and extrusive), metamorphic (gneiss and schist) and plutonic (granite mainly) rocks. In the middle part of the catchments, marine and continental

sedimentary rocks of various ages separated by fault systems are found. In contrast, eastern coastal plains are mainly composed of Tertiary and Quaternary marine and continental sedimentary rocks.

Woodland is the main land use in this area (covering 68–78% of the total surface), followed by cropland (10–13%). The region is exposed to typhoons and spring snowmelt events leading to severe soil erosion and subsequent export of sediment in rivers (Chartin et al., 2013; Evrard et al., 2013). We therefore conducted three sampling campaigns after each of those major hydro-sedimentary events (i.e., Nov. 2011, April 2012, and Nov. 2012).

2.2. Sample collection, preparation and description of experiments.

After the accident, the Ministry of Education, Culture, Sports, Science and Technology in Japan (MEXT) supervised the sampling of soils at 2200 sites located within a radius of approximately 100 km around FDNPP in June and July 2011, and the analysis of their activities in several radionuclides contained in their 5-cm upper layer (^{110m}Ag activities were only provided for a selection of 345 sites; MEXT 2011).

Based on this dataset, a map of ^{110m}Ag:^{137}Cs activity ratio values in soils was drawn (Chartin et al., 2013). Unlike ^{134}Cs:^{137}Cs activity ratio, it revealed the presence of different contamination patterns across the area (Fig. 3), with lower values across mountains and higher values in the coastal lowlands.

The relatively low abundance of ^{110m}Ag in soils of the study area in Fukushima (activities ranging between 2 – 2400 Bq kg^{-1}) compared to those in ^{134}Cs and ^{137}Cs (500 – 1,245,000 Bq kg^{-1}) required relatively long counting times and the use of low-background high-resolution detectors to allow its detection. This probably explains why this radioisotope has not been

136 measured more widely during the months that followed the accident. We therefore decided
137 to restrict this study to the main contamination plume (Table 2) in order to minimize
138 uncertainties associated with ^{110m}Ag measurements.

139 **A. Behaviour of ^{110m}Ag in soils**

140 *Experiment 1 – Affinity with different grain size fractions*

141 Four soil samples (~300g/sample – Soil 1 to Soil 4 - Fig. 3) were collected using non-metallic
142 trowels in different parts of the contamination plume where ^{110m}Ag:^{137}Cs activity ratio varies
143 from 0.002 to 0.008. After drying at 40°C, samples were dry-sieved to 1mm, 500µm, 250µm
144 and 63µm using an automatic device, in order to measure the respective activities present in
145 the different grain size fractions.

146 *Experiment 2 – Migration in soil*

147 To investigate the potential migration of radionuclides with depth in soil, gamma
148 measurements were conducted on each 2-mm increment of the uppermost 2-cm of a soil
149 profile sampled near Kawamata city (Profile - Fig. 3). Soil layers were collected using a
150 scraper plate composed by a metal frame and a metal plate (Loughran et al., 2002; Kato et
151 al., 2012b). To avoid contamination by top layers, a spray glue was used to fix the sample.

152 ^{137}Cs concentration in undisturbed Japanese soils is expected to show an exponential decline
153 with depth (Kato et al., 2012b; Koarashi et al., 2012; Matsunaga et al., 2013). Cumulative
154 inventory can be expressed as described in Eq. (1):

155 $$I_{(x)} = I_t \left(1 - \exp^{-x/h_0}\right) \quad (1)$$

Where $\mathbf{I_{(x)}}$ is the radiocesium inventory ($Bq.m^{-2}$) at the **x** ($kg.m^{-2}$) depth, $\mathbf{I_t}$ is the total radiocesium inventory and $\mathbf{h_0}$ is the relaxation mass depth ($kg.m^2$), an index characterising the radiocesium penetration in the soil. In order to use this formula, we calculated the ^{137}Cs inventory using ^{137}Cs activities ($Bq.kg^{-1}$) (Lee et al., 2013) at the successive (x) depths (Eq. 2):

$$I(x) = \rho(x) * h(x) * A(x) \quad (2)$$

Where **ρ** is the dry bulk density ($g.m^{-3}$), **h** is the thickness (cm) of the layer and **A** the activity ($Bq.kg^{-1}$) of this layer.

B. Behaviour of ^{110m}Ag in rivers

Experiment 3 – Activities in sediment sequences accumulated in reservoirs

During the November 2012 fieldwork campaign, we had the opportunity to collect samples of the different layers representative of the deep sediment sequence that accumulated behind Tetsuzen dam on Ota River (1.6 m) and behind Takanokura dam on Mizunashi River (Nitta catchment) (0.5 m) in order to investigate ^{110m}Ag behaviour in respectively 9 and 7 different layers (Dam Sed 1 and Dam Sed 2 - Fig. 3). We removed the exposed sediment lateral surface to avoid artificial sample contamination during fieldwork.

Particle size of the samples was measured using a SALD-3100 Laser (Shimadzu Co., Ltd., Kyoto, Japan) following standard procedures. The particles were classified into 42 size ranges between 0.05 and 450µm. The surface specific area was estimated using the density of quartz (2.65g cm^{-3}) and assuming that particles were spherical (Santamarina and Klein, 2002). Grain size distribution was corrected using sieving data for classes >450µm, and final classes were reclassified according to the grain-size ranges proposed by AFNOR X 316107 (i.e., clay <2µm, 2 µm < silt < 50µm, 50µm < sand < 2mm).

178 *Experiment 4 – Impact of typhoon and snowmelt on activities in river drape sediment*

179 A last experiment was conducted in upper parts of the Nitta River catchment (with
180 elevation > 400m), where the ^{110m}Ag:^{137}Cs activity ratio in soils is low but overall radioactive
181 contamination is high. This area was impacted by summer typhoons and spring snowmelt
182 events that generated soil erosion on hillslopes and led to an increase in river discharge
183 (Fukuyama et al., 2005; Iida et al., 2012; Ueda et al., 2013). Sediment drape deposits (SDD)
184 were selected as an alternative to suspended sediment in order to increase the spatial
185 coverage of the survey within the catchments, and to avoid the logistical problems
186 associated with the collection of suspended sediment in rivers. Olley et al. (2013)
187 demonstrated that sediment source apportionment conducted on SDD and suspended
188 matters showed similar results. To prepare a representative sample, five to ten subsamples
189 that are likely to have deposited after the last major flood were collected at several locations
190 selected randomly down to the underlying coarser cobble or gravel layer across a $10m^2$
191 surface. Sediment drape deposits are likely to integrate deposits of the last hydro-
192 sedimentary events of low to intermediate magnitude (Evrard et al., 2011) even though the
193 occurrence of large floods probably leads to a complete flush of the system justifying the
194 relevance of conducting field surveys to collect sediment drape deposits as frequently as
195 possible.

196 Activities were measured in 4 representative SDD samples collected at the same location
197 during the four successive fieldwork campaigns (SDD 1 to SDD 4 - Fig. 3). Grain size
198 measurements were conducted by following the same protocol as described for Experiment
199 3.

200 2.3 Gamma spectrometry measurements

Before measurement, samples were dried at 40°C (105°C for soil), ground to a fine powder and then packed into 15mL polyethylene specimen cups. Radionuclide activities (^{134}Cs, ^{137}Cs, ^{110m}Ag) in all samples were determined by gamma spectrometry using very low-background coaxial N- and P-types HPGe detectors (Canberra / Ortec). Counting times of soil and sediment samples varied between 8×10^4 and 200×10^4 s to allow the detection of ^{110m}Ag, which was present in much lower activities in the samples (2–2400 Bq.kg^{-1}) than ^{134}Cs and ^{137}Cs (500–1,245,000 Bq.kg^{-1}).

The ^{137}Cs activities were measured at the 661 keV emission peak. The ^{134}Cs ($T_{1/2}$ = 2y) activities were calculated as the mean of activities derived from measurements conducted at 604 keV and 795 keV (^{228}Ac activities being negligible compared to ^{134}Cs activities) as both peaks are associated with the largest gamma emission intensities of this radionuclide.

The presence of ^{110m}Ag was confirmed by the detection of an emission peak at 885 keV (as the peak associated with the largest emission intensity at 658 keV was masked by the 661-keV peak of ^{137}Cs). Minimum detectable activities in ^{110m}Ag for 24h counting times reached 2 Bq.kg^{-1}. Detection of ^{110m}Ag was considered relevant when the 885 keV peak was present. Because of their low level, activities in ^{110m}Ag were associated with larger uncertainties than activities in ^{137}Cs. Counting efficiencies and quality assurance were conducted using internal and certified International Atomic Energy Agency (IAEA) reference materials prepared in the same specimen cups as the samples. Uncertainties on results were estimated by combining counting statistics and calibration uncertainties. Summing and self-absorption effects were taken into account by analysing standards with similar densities and characteristics as the collected samples. All radionuclide activities were decay corrected to the date of 14 March 2011 corresponding to the date of the first radionuclide deposits on soils. Most of them

were estimated to have deposited on 15 March in Fukushima Prefecture (Kinoshita et al., 2011; Shozugawa et al., 2012).

3. Results and discussion

A. Behaviour of ^{110m}Ag in soils

Experiment 1 – Affinity with different grain size fractions (Soil 1 to Soil 4)

During this experiment, ^{110m}Ag activities could only be detected in all fractions for 2 of the 4 analysed samples (Soil 1 and Soil 2 – Fig. 3) as a result of low $T_{1/2}$ and low ^{110m}Ag initial deposition level. Samples were indeed collected in the vicinity of the main contamination plume as access to the most affected area was restricted by Japanese authorities. It also has been detected in the finest fraction of the Soil 4 sample. Fig. 4 describes the distribution of ^{110m}Ag and ^{137}Cs radionuclides in the different grain size fractions of Soil 1 and Soil 2 samples.

Activity distribution is similar for both radionuclides and the major part (from 33% to 65%) of their activity was measured in the finest fraction (<63µm; Table 3). We could therefore not detect any difference in the particle-size effects of adsorption between both radionuclides.

This finding is crucial in order to use the ^{110m}Ag:^{137}Cs activity ratio to track the dispersion of contaminated particles in catchments, as the finest particles are the most susceptible to be eroded and redistributed (Motha et al., 2002).

Experiment 2 – Migration in soil (Profile)

Activities measured in the uppermost part of the soil profile (Fig. 3) confirmed the low mobility of ^{134}Cs, ^{137}Cs and ^{110m}Ag (Table 4). The bulk of their inventories (≈80%) were contained in the first layers (0 – 8 mm) and decreased rapidly with depth (Fig. 5).

245 The ^{137}Cs total inventory reached about 417 kBq.m^{-2} and the relaxation mass depth h_0 was
246 7.1kg.m^{-2} for ^{137}Cs (Fig. 6). This value is close to the one found by Kato et al. (2012b) in a
247 cultivated soil (9.1 kg.m^{-2}) in the vicinity of our sampling site. This value also remained in the
248 same order of magnitude as in several cultivated soils investigated by Ivanov (Ivanov et al.,
249 1997) near the Chernobyl Power Plant (ranging from 5.6 to 9.1 kg.m^{-2}).

250 In order to compare the behaviour of both radionuclides, we calculated in the same way the
251 relaxation mass depth for the ^{110m}Ag and found 7.6 kg.m^{-2} with a total ^{110m}Ag inventory value
252 of 1 kBq.m^{-2}, showing that penetration of both radionuclides in the soil was similar.

253 Our results are consistent with the ones provided by other studies that investigated the
254 behaviour of the same radionuclides in soils. Alloway (1995) showed that ^{110m}Ag is not
255 mobile as it is the case for ^{137}Cs (Sawi-iney, 1972; Spezzano, 2005) and they both remain in
256 the uppermost 5cm of the soil (Handl et al., 2000; Kato et al., 2012b; Shang and Leung, 2003)

257 We investigated the migration of radionuclides in a profile of bare soil, but the transposition
258 of those results to soils covered with vegetation is not straightforward, as the radionuclide
259 interception and migration processes were reported to play a major role in forested
260 environments (Kato et al., 2012a). Furthermore, Martin et al. (1989) reported that during the
261 first months that followed Chernobyl fallout, ^{110m}Ag required more time to migrate from
262 grass to soil (50% reduction) than ^{137}Cs (90% reduction) due to foliar leaching. However, this
263 effect should have remained limited in Fukushima, as most cultivated soils (i.e., paddy fields)
264 were found to be bare when atmospheric fallout occurred in March 2011.

These results confirm the low mobility of ^{110m}Ag in cultivated soils. As it remained concentrated in the first layers, it could be rapidly redistributed across hillslopes as a consequence of runoff and soil erosion.

C. Behaviour of ^{110m}Ag in rivers

Experiment 3 – Activities in sediment sequences accumulated in reservoirs (Dam Sed 1 & 2)

The pH measured in the four investigated rivers varied between 5.0 and 6.0. It was demonstrated in the literature that pH plays a major role on ^{110m}Ag behaviour in both soil and water. Its mobility in soils (Khan et al., 1982; Shang and Leung, 2003) increases when pH raises and its affinity for suspended particulate matter (SPM) rises when pH exceeds 7, to reach maximum values at a pH of 9 (Fukai and Murray, 1974; Murray and Murray, 1972). In contrast, ^{137}Cs was shown not to be affected by a pH variation (Adam et al., 2001). Because the observed pH values remained significantly lower than 7, ^{110m}Ag behaviour and ^{110m}Ag:^{137}Cs activity ratio were not expected to be affected by pH variations in Fukushima rivers.

Analysis of the two sediment profiles (Dam Sed 1 and 2 – Fig. 3) tends to confirm the similar post-depositional behaviour of the radionuclides (Figs. 7 and 8). Their activities were concentrated in the top of the profile (Tables 5 and 6), and most likely resulted from deposition of sediment eroded after the initial radionuclide fallout in March 2011. Before the FDNPP accident, ^{137}Cs activities in sediment were generally lower than 100Bq/kg in Japanese soils (Fukuyama et al., 2005), which corresponds to activities found in deeper layers of sediment accumulated behind Tetsuzen dam (Dam Sed 1). Higher contamination in lower layers in the second profile (> 500Bq/kg) most likely resulted from contamination

originating from upper levels during sampling (scraping). However, this will not impact the conclusions drawn from this experiment as they strictly focus on the observations made on the top layers.

In Tetsuzen dam sediment (Dam Sed 1), a lower activity was measured in the surface layer than in the underlying layer suggesting that a minimum of two significant erosion events had supplied contaminated sediment to the reservoir by November 2012 (Fig. 7; Table 5). Also, $^{110m}Ag/^{137}Cs$ activity ratio remained constant for these layers. Furthermore, a significant difference in particle size between the first two layers and the third layer confirms the occurrence of an intense erosion event, probably during the dam release that was carried out during the period of heavy typhoons that took place during summer in 2011. Based on this information, sedimentation rates were estimated to 20cm yr^{-1} in Tetsuzen dam, and to 5cm yr^{-1} in Takanokura dam.

The similar percentage of radionuclide inventories found in the successive layers and the calculation of constant $^{110m}Ag:^{137}Cs$ activity ratios confirmed that ^{110m}Ag and ^{137}Cs have a similar behaviour with regard to their adsorption onto soil particles and sediment. This result was expected owing to the high distribution coefficients reported in the literature for both Cs and Ag (Ciffroy et al., 2001; Fournier-Bidoz and Garnier-Laplace, 1994). K_d values remaining in the same order of magnitude were estimated for both radionuclides in winter and summer (i.e. $K_{dCs-}{}^{137}$: 0.1-100; $K_{dAg-}{}^{110m}$: 1-100). Ciffroy et al. (2001) also quantified the kinetics of the adsorption and desorption of these radionuclides in freshwater systems, and concluded to their similar behaviour. Fournier-Bidoz and Garnier-Laplace (1994) and Garnier et al. (2006) showed that ^{110m}Ag has a strong affinity for river SPM and especially for their

clay fraction. A large number of studies demonstrated that Cs has the same behaviour (Ojima et al. , 1965 in Ancelin et al., 1979; Garnier-Laplace et al., 1994). He and Walling (1996) confirmed that ^{137}Cs affinity increases with specific surface area in the case of a uniform contamination of the soils. Guéguéniat et al. (1976) reported similar results for ^{110m}Ag.

Experiment 4 – Impact of typhoon and snowmelt

During the three successive sampling campaigns that followed the succession of snowmelt and typhoon events, the inventories of ^{110m}Ag and ^{137}Cs measured in sediment drape deposits collected systematically at four sampling points in the upper part of the Nitta catchment (Fig. 3) showed similar patterns (Fig. 9). As expected, samples collected close to the catchment headwaters (SDD 1 and SDD 4) showed a decrease in contamination throughout time, probably due to the flush of the most contaminated material during high water flows (Table 7). In contrast, the samples collected at the 2 downstream locations (especially SDD 3) were associated with a slight temporal increase in contamination of ^{137}Cs that may be explained by a supply of upstream – more contaminated – material. This explanation is consistent with the fact that ^{110m}Ag:^{137}Cs activity ratio measured in sediment remained in the same order of magnitude as the ratio measured in soils of this upper part of the Nitta catchment (Table 8).

An alternative explanation to the activity increase observed throughout time is that the grain size of particles could have changed from one campaign to the next, explaining the observed differences in contamination. Calculation of surface specific area (SSA) shown in Fig. 9 shows that this might be the case for sample SDD 3 (with an enrichment in fine particles throughout time), but not for sample SDD 2 (SSA remaining constant in time).

Because of different experimental conditions (non-homogeneous fallout deposition and high radionuclide activities), our results plotted on Fig. 10 do not show a power function as found by He and Walling (1996) but they display instead a linear function for both ^{137}Cs ($r^2 = 0.89$) and ^{110m}Ag ($r^2 = 0.91$) that is strongly correlated with the SSA.

This tends to confirm the similar behaviour for both radionuclides, although particle-size effects and fractionation could have occurred, given that erosion and transport in rivers are obviously selective to finer particles. Consequently, these results confirmed the relevance of using of ^{110m}Ag:^{137}Cs activity ratio to investigate the dispersion and redistribution of contamination along rivers.

Conclusions

Silver-110m (^{110m}Ag) is an anthropogenic radionuclide that is produced continuously by nuclear power plants (NPP) in normal conditions, but investigations regarding its behaviour in the environment are rare despite the potentially important radioecological implications of its accidental release into the environment. In the Fukushima NPP post-accidental context, the interest to conduct field studies on the behaviour of ^{110m}Ag was reinforced by the fact that initial deposits displayed ^{110m}Ag:^{137}Cs activity ratios that varied across space within the main radioactive contamination plume. This study showed that ^{137}Cs and ^{110m}Ag were strongly sorbed by the finest particle fractions (i.e., clay or silt), and that the bulk of their inventory was stored in the uppermost part of soil profiles (i.e., <2 cm), confirming that the in-depth mobility was not significant during the two years following the accident. In addition to this fine particle reactivity, we showed that soil erosion and sediment transport in catchments that mobilize preferentially the finest particle fractions did not induce different fractionation effects for both radionuclides. This study therefore confirmed the relevance of

using this ratio to track the dispersion of contaminated material along coastal rivers draining this area. In future, due to the rapid decay of radiosilver and its initially relatively low fallout level, extraction methods could be used in order to measure precisely radiosilver and continue to investigate its behaviour and the dispersion of contaminated sediment along rivers.

Acknowledgements

This work was a part of the TOFU (Tracing the environmental consequences of the Tohoku earthquake-triggered tsunami and Fukushima accident) project, funded by the joint French National Research Agency-Flash Japon (ANR- 11-JAPN-001) and Japan Science and Technology agency/J-RAPID programme. H. L. received a PhD fellowship from CEA (Commissariat à l'Energie Atomique et aux Energies Alternatives).

References

Adam, C., Baudin, J.P., Garnier-laplace, J., 2001. Kinetics of Ag-110m, Co-60, Cs-137 and Mn-54 bioaccumulation from water and depuration by the Crustacean Daphnia magna. Water Air Soil Pollut. 125, 171–188.

Ancelin, J., Guéguéniat, P., Germain, P., 1979. Radioécologie marine, étude du devenir des radionucléides rejetés en milieu marin et application à la radioprotection, Eyrolles. ed. Paris.

Beresford, N.A., Crout, N.M.J., Mayes, R.W., Howard, B.J., Lamb, C.S., 1998. Dynamic distribution of radioisotopes of cerium, ruthenium and silver in sheep tissues. J. Environ. Radioact. 38, 317–338.

Bryan, G.W., 1971. Effects of heavy metals (other than Mercury) on marine and estuarine organisms. Proc. R. Soc. Ser. B - Biol. Sci. 177, 389.

Bryan, G.W., Langston, W.J., 1992. Bioavailability, accumulation and effects of heavy metals in sediments with special reference to United Kingdom estuaries: a review. Environ. Pollut. 76, 89–131.

Buesseler, K.O., Jayne, S.R., Fisher, N.S., Rypina, I.I., Baumann, H., Baumann, Z., Breier, C.F., Douglas, E.M., George, J., Macdonald, A.M., Miyamoto, H., Nishikawa, J., Pike, S.M., Yoshida, S., 2012. Fukushima-derived radionuclides in the ocean and biota off Japan. Proc. Natl. Acad. Sci. U. S. A. 5984-5988, 1–7.

Calmon, P., Garnier-Laplace, J., 2002. Fiche radionucléide - Argent-110m et environnement. IRSN 15.

390 Chartin, C., Evrard, O., Onda, Y., Patin, J., Lefèvre, I., Ottlé, C., Ayrault, S., Lepage, H., Bonté,
391 P., 2013. Tracking the early dispersion of contaminated sediment along rivers draining
392 the Fukushima radioactive pollution plume. Anthropocene 1, 23-34.

393 Chelet, Y., 2006. La radioactivité - Manuel d'initiation, Nucléon. ed.

394 Chino, M., Nakayama, H., Nagai, H., Terada, H., Katata, G., Yamazawa, H., 2011. Preliminary
395 Estimation of Release Amounts of 131 I and 137 Cs Accidentally Discharged from the
396 Fukushima Daiichi Nuclear Power Plant into the Atmosphere. J. Nucl. Sci. Technol. 48,
397 1129–1134.

398 Ciffroy, P., Garnier, J.-M., Pham, M.K., 2001. Kinetics of the adsorption and desorption of
399 radionuclides of Co, Mn, Cs, Fe, Ag and Cd in freshwater systems: experimental and
400 modelling approaches. J. Environ. Radioact. 55, 71–91.

401 Ciffroy, P., Siclet, F., Damois, C., Luck, M., Duboudin, C., 2005. A dynamic model for assessing
402 radiological consequences of routine releases in the Loire river: parameterisation and
403 uncertainty/sensitivity analysis. J. Environ. Radioact. 83, 9–48.

404 Evrard, O., Navratil, O., Ayrault, S., Ahmadi, M., Némery, J., Legout, C., Lefèvre, I., Poirel, A.,
405 Bonté, P., Esteves, M., 2011. Combining suspended sediment monitoring and
406 fingerprinting to determine the spatial origin of fine sediment in a mountainous river
407 catchment. Earth Surf. Process. Landforms 36, 1072–1089.

408 Evrard, O., Chartin, C., Onda, Y., Patin, J., Lepage, H., Lefèvre, I., Ayrault, S., Ottlé, C., Bonté,
409 P. (2013). Evolution of radioactive dose rates in fresh sediment deposits along rivers
410 draining Fukushima contamination plume. Scientific Reports 3, 3079.

411 Eyrolle, F., Radakovitch, O., Raimbault, P., Charmasson, S., Antonelli, C., Ferrand, E., Aubert,
412 D., Raccasi, G., Jacquet, S., Gurriaran, R., 2012. Consequences of hydrological events on
413 the delivery of suspended sediment and associated radionuclides from the Rhône River
414 to the Mediterranean Sea. J. Soils Sediments 12, 1479–1495.

415 Fournier-Bidoz, V., Garnier-laplace, J., 1994. Etude bibliographique sur les échanges entre
416 l'eau les matières en suspension et les sédiments des principaux radionucléides rejetés
417 par les centrales nucléaires, Radioprotection. IPSN.

418 Fournier-Bidoz, V., Garnier-laplace, J., Baudin, J., 1997. État des connaissances sur les
419 échanges entre l'eau, les matières en suspension et les sédiments des principaux
420 radionucléides rejetés par les centrales nucléaires en eau douce. Radioprotection 3, 49–
421 71.

422 Fukai, R., Murray, C., 1974. Environmental behavior of radiocobalt and radiosilver released
423 from nuclear power stations into aquatic systems. Radioact. Sea 40, 217–242.

424 Fukuda, T., Kino, Y., Abe, Y., Yamashiro, H., Kuwahara, Y., Nihei, H., Sano, Y., Irisawa, A.,
425 Shimura, T., Fukumoto, Motoi, Shinoda, H., Obata, Y., Saigusa, S., Sekine, T., Isogai, E.,
426 Fukumoto, Manabu, 2013. Distribution of artificial radionuclides in abandoned cattle in
427 the evacuation zone of the Fukushima Daiichi nuclear power plant. PLoS One 8, e54312.

428 Fukuyama, T., Takenaka, C., Onda, Y., 2005. 137Cs loss via soil erosion from a mountainous
429 headwater catchment in central Japan. Sci. Total Environ. 350, 238–47.

Garnier, J.-M., Ciffroy, P., Benyahya, L., 2006. Implications of short and long term (30 days) sorption on the desorption kinetic of trace metals (Cd, Zn, Co, Mn, Fe, Ag, Cs) associated with river suspended matter. Sci. Total Environ. Environ. 366, 350–60.

Guéguéniat, P., Gandon, R., Hémon, G., Philippot, J.C., 1976. Méthode de mesure d'éléments traces dans l'eau de mer par activation neutronique. Cas particulier des isotopoes stables de produits de fission. Meas. Detect. Control Environ. Pollut. IAEA-SM, 206/28.

Handl, J., Kallweit, E., Henning, M., Szwec, L., 2000. On the long-term behaviour of 110mAg in the soil–plant system and its transfer from feed to pig. J. Environ. Radioact. 48, 159–170.

He, Q., Walling, D., 1996. Interpreting particle size effects in the adsorption of 137 Cs and unsupported 210 Pb by mineral soils and sediments. J. Environ. Radioact. 30, 117–137.

IAEA, 1998. Radiological characterization of shut down nuclear reactors for decommissioning purposes. IAEA, Vienna, Tech. Rep 389, 184.

Iida, T., Kajihara, A., Okubo, H., Okajima, K., 2012. Effect of seasonal snow cover on suspended sediment runoff in a mountainous catchment. J. Hydrol. 428-429, 116–128.

Ivanov, Y., Lewyckyj, N., Levchuk, S., 1997. Migration of 137 Cs and 90 Sr from chernobyl fallout in Ukrainian, Belarussian and Russian soils. J. Environ. Qual. 35, 1–21.

Kato, H., Onda, Y., Gomi, T., 2012a. Interception of the Fukushima reactor accident derived 137Cs, 134Cs and 131I by coniferous forest canopies. Geophys. Res. Lett. 39, L20403.

449 Kato, H., Onda, Y., Teramage, M., 2012b. Depth distribution of 137Cs, 134Cs, and 131I in soil
450 profile after Fukushima Dai-ichi Nuclear Power Plant Accident. J. Environ. Radioact. 111,
451 59–64.

452 Khan, S., Nandan, D., Khan, N.N., 1982. The mobility of some heavy metals through Indian
453 Red Soil. Environ. Pollut. Ser. B, Chem. Phys. 4, 119–125.

454 Khangarot, B., Ray, P., 1987. Correlation between heavy metal acute toxicity values
455 inDaphnia magna and fish. Bull. Environ. Contam. Toxicol. 38, 722–726.

456 Kinoshita, N., Sueki, K., Sasa, K., Kitagawa, J., Ikarashi, S., Nishimura, T., Wong, Y.-S., Satou,
457 Y., Handa, K., Takahashi, T., Sato, M., Yamagata, T., 2011. Assessment of individual
458 radionuclide distributions from the Fukushima nuclear accident covering central-east
459 Japan. Proc. Natl. Acad. Sci. U. S. A. 108, 19526–9.

460 Koarashi, J., Atarashi-Andoh, M., Matsunaga, T., Sato, T., Nagao, S., Nagai, H., 2012. Factors
461 affecting vertical distribution of Fukushima accident-derived radiocesium in soil under
462 different land-use conditions. Sci. Total Environ. Environ. 431, 392–401.

463 Lee, S.H., Oh, J.S., Lee, J.M., Lee, K.B., Park, T.S., Lujaniene, G., Valiulis, D., Sakalys, J., 2013.
464 Distribution characteristics of (137)Cs, Pu isotopes and (241)Am in soil in Korea. Appl.
465 Radiat. Isot. In press.

466 Martin, C.J., Heaton, B., Thompson, J., 1989. Cesium-137, 134Cs and 110mAg in lambs
467 grazing pasture in NE Scotland contaminated by Chernobyl fallout. Health Phys. 56,
468 459–64.

469 Martin, T.R., Holdich, D.M., 1986. The acute lethal toxicity of heavy metals to peracarid
470 crustaceans. Water Res. 20, 1137–1147.

471 Matsunaga, T., Koarashi, J., Atarashi-Andoh, M., Nagao, S., Sato, T., Nagai, H., 2013.
472 Comparison of the vertical distributions of Fukushima nuclear accident radiocesium in
473 soil before and after the first rainy season, with physicochemical and mineralogical
474 interpretations. Sci. Total Environ. Environ. 447C, 301–314.

475 MEXT, 2011. Preparation of Distribution Map of Radiation Doses (Map of Tellure 129 and
476 Silver 110m Concentration in Soil).

477 Murray, C.N., Murray, L., 1972. Adsorption-desorption equilibria of some radionuclides in
478 sediment-fresh-water and sediment-sea water systems. Radioact. Contam. Mar.
479 Environ. 105–122.

480 Olley, J., Brooks, A., Spencer, J., Pietsch, T., Borombovits, D., 2013. Subsoil erosion
481 dominates the supply of fine sediment to rivers draining into Princess Charlotte Bay,
482 Australia. J. Environ. Radioact. 124C, 121–129.

483 Oughton, D., 1989. The environmental chemistry of radiocaesium and other nuclides.
484 University of Manchester.

485 Petit, G., Douysset, G., Ducros, G., Gross, P., Achim, P., Monfort, M., Raymond, P., Pontillon,
486 Y., Jutier, C., Blanchard, X., Taffary, T., Moulin, C., 2012. Analysis of Radionuclide
487 Releases from the Fukushima Dai-Ichi Nuclear Power Plant Accident Part I. Pure Appl.
488 Geophys.

489 Ratte, H.T., 1999. Bioaccumulation and toxicity of silver compounds: A review. Environ.
490 Toxicol. Chem. 18, 89–108.

491 Santamarina, J., Klein, K., 2002. Specific surface: determination and relevance. Can. Geotech.
492 241, 233–241.

493 Shang, Z.R., Leung, J.K.C., 2003. 110m Ag root and foliar uptake in vegetables and its
494 migration in soil. J. Environ. Radioact. 65, 297–307.

495 Shozugawa, K., Nogawa, N., Matsuo, M., 2012. Deposition of fission and activation products
496 after the Fukushima Dai-ichi nuclear power plant accident. Environ. Pollut. 163, 243–7.

497 Stohl, A., Seibert, P., Wotawa, G., Arnold, D., Burkhart, J.F., Eckhardt, S., Tapia, C., Vargas, A.,
498 Yasunari, T.J., 2012. Xenon-133 and caesium-137 releases into the atmosphere from the
499 Fukushima Dai-ichi nuclear power plant: determination of the source term, atmospheric
500 dispersion, and deposition. Atmos. Chem. Phys. 12, 2313–2343.

501 Tanaka, K., Sakaguchi, A., Kanai, Y., Tsuruta, H., Shinohara, A., Takahashi, Y., 2012.
502 Heterogeneous distribution of radiocesium in aerosols, soil and particulate matters
503 emitted by the Fukushima Daiichi Nuclear Power Plant accident: retention of micro-
504 scale heterogeneity during the migration of radiocesium from the air into ground and
505 rive. J. Radioanal. Nucl. Chem. 295, 1927–1937.

506 Tateda, Y., Tsumune, D., Tsubono, T., 2013. Simulation of radioactive cesium transfer in the
507 southern Fukushima coastal biota using a dynamic food chain transfer model. J.
508 Environ. Radioact. 124, 1–12.

509 Tazoe, H., Hosoda, M., Sorimachi, A., Nakata, A., Yoshida, M. a, Tokonami, S., Yamada, M.,
510 2012. Radioactive pollution from Fukushima Daiichi nuclear power plant in the
511 terrestrial environment. Radiat. Prot. Dosimetry 152, 198–203.

512 Ueda, S., Hasegawa, H., Kakiuchi, H., Akata, N., Ohtsuka, Y., Hisamatsu, S., 2013. Fluvial
513 discharges of radiocaesium from watersheds contaminated by the Fukushima Dai-ichi
514 Nuclear Power Plant accident, Japan. J. Environ. Radioact. 118, 96–104.

515 Vuković, Ž., 2002. Environmental impact of radioactive silver released from nuclear power
516 plant. J. Radioanal. Nucl. Chem. 254, 637–639.

517 Watanabe, T., Tsuchiya, N., Oura, Y., Ebihara, M., 2012. Distribution of artificial radionuclides
518 (110mAg, 129mTe, 134Cs, 137Cs) in surface soils from Miyagi Prefecture, northeast
519 Japan, following the 2011 Fukushima Dai-ichi nuclear power. Geochem. J. 46, 279–285.

520 Winiarek, V., Bocquet, M., Saunier, O., Mathieu, A., 2012. Estimation of errors in the inverse
521 modeling of accidental release of atmospheric pollutant: Application to the
522 reconstruction of the cesium-137 and iodine-131 source terms from the Fukushima
523 Daiichi power plant. J. Geophys. Res. 117, 1–16.

524 Yasunari, T., Stohl, A., Hayano, R.S., Burkhart, J.F., Eckhardt, S., 2011. Cesium-137 deposition
525 and contamination of Japanese soils due to the Fukushima nuclear accident. Proc. Natl.
526 Acad. Sci. U. S. A. 108, 19530–4.

527

528

Figure captions

Figure 1. Number of publications per year between 1937 and 2013 based on a search in the Web of Knowledge citation index, using “radiosilver” (or “Ag-110m” » or “^{110m}Ag”) and “environment” as topic keywords (22 July 2013).

Figure 2. Location of the main radiocaesium (^{134}Cs + ^{137}Cs) contamination plume in Fukushima Prefecture, northeastern Japan (derived from MEXT data decay-corrected to June 2011).

Figure 3. Location of the samples collected across the main contamination plume of Fukushima Prefecture. Background map corresponds to ^{110m}Ag:^{137}Cs activity ratio based on data measured in Fukushima Prefecture by MEXT in June 2011 (activities decay-corrected to 14 June 2011). SDD: sediment drape deposits, Dam Sed 1: sediment collected in Tetsuzen dam, Dam Sed 2: sediment collected in Takanokura dam; FDNPP: Fukushima Dai-ichi Nuclear Power Plant.

Figure 4. Percentage of total activity in ^{110m}Ag and ^{137}Cs in four particle size classes (d = diameter) for two soil samples (Soil 1 and Soil 2 - see the location of sampling sites on Figure 3).

Figure 5. Radionuclide inventory (%) in successive 2-mm increment layers along a bare soil profile (Profile - see the location of sampling sites on Figure 3).

Figure 6. Distribution of ^{137}Cs inventory (%) in the bare soil profile as measured by gamma spectrometry and fitted using Eq. (1), as a function of mass depth (kg.m^{-2}) (Profile - see the location of sampling sites on Figure 3).

Figure 7. Sediment profile accumulated in Yokokawa reservoir on the Ota River (Dam Sed 1 – see the location of sampling sites on Figure 3) – a) Picture of the profile: the limits of the numbered sampled layers are represented with horizontal lines - b) Anthropogenic radionuclide inventories (%) in the successive layers of the profile (mm) – c) Grain size composition of the different layers.

Figure 8. Sediment profile accumulated behind Takanokura dam on the Mizunashi River (Nitta catchment – Dam Sed 2 – see the location of sampling sites on Figure 3) – a) Picture of the profile: the limits of the numbered sampled layers are represented with horizontal lines - b) Activity in anthropogenic radionuclides in the successive layers of the profile – c) Grain size composition of the different layers.

Figure 9. Evolution of the ^{137}Cs and ^{110m}Ag contamination inventory (%) and specific surface area (SSA) ($m^2.g^{-1}$) of sediment drape deposits collected in the upper part of the Nitta River catchment during the campaigns of Nov 2011, April 2012 and Nov 2012 (SDD 1 to SDD 4 – see the location of sampling sites on Figure 3).

Figure 10. Relationships between ^{137}Cs and ^{110m}Ag activities ($Bq.kg^{-1}$) and specific surface area ($m^2.g^{-1}$) in sediment drape deposits collected in the upper part of the Nitta River catchment during the campaigns of Nov 2011, April 2012 and Nov 2012 (SDD 1 to SDD 4 – see the location of sampling sites on Figure 3).

fig1.docx

Click here to download Figure: FIG1.docx

Figure 1.

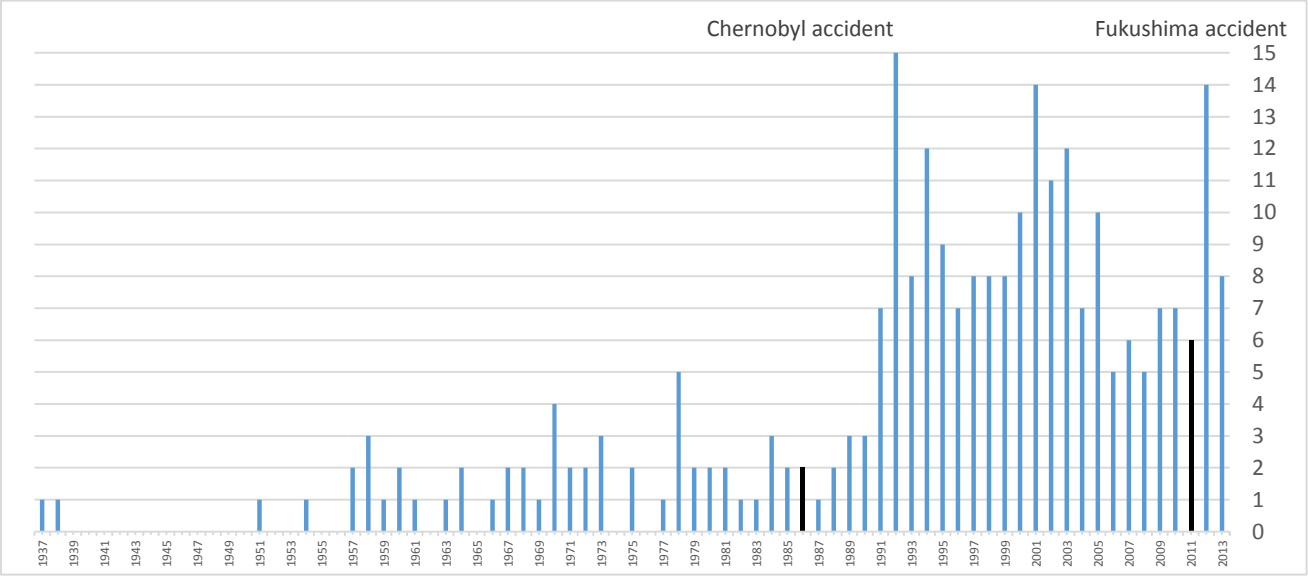


fig2.docx

Click here to download Figure: FIG2.docx

Figure 2.

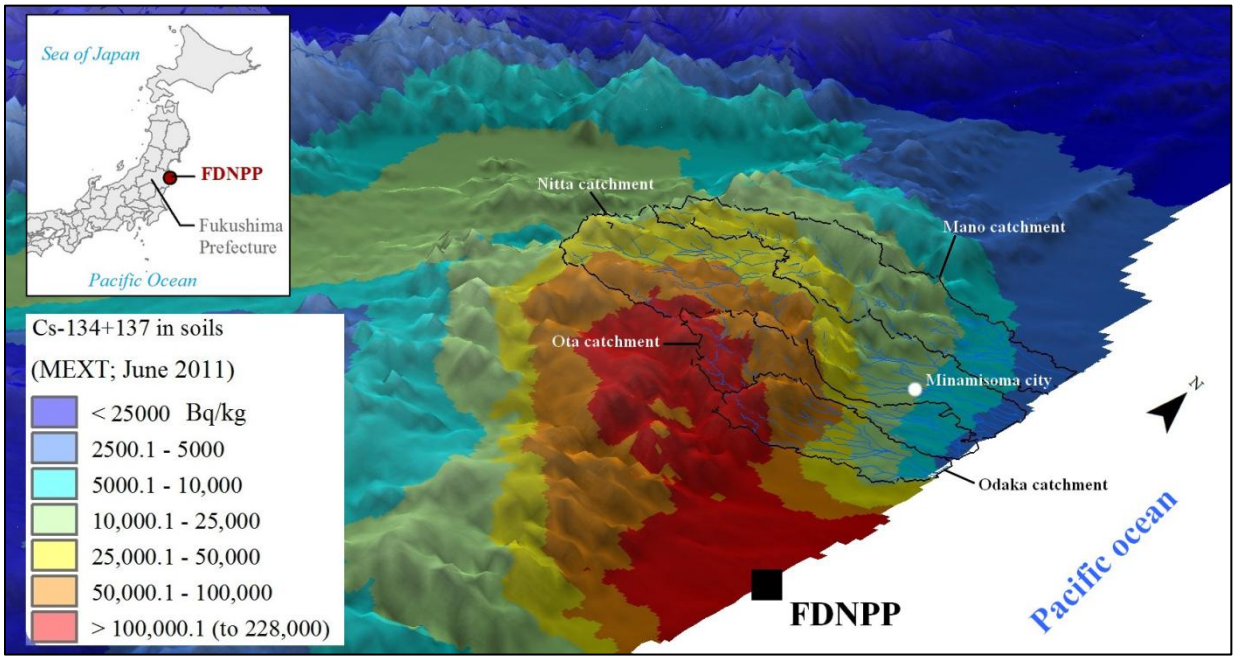


fig3.docx

Click here to download Figure: FIG3.docx

Figure 3.

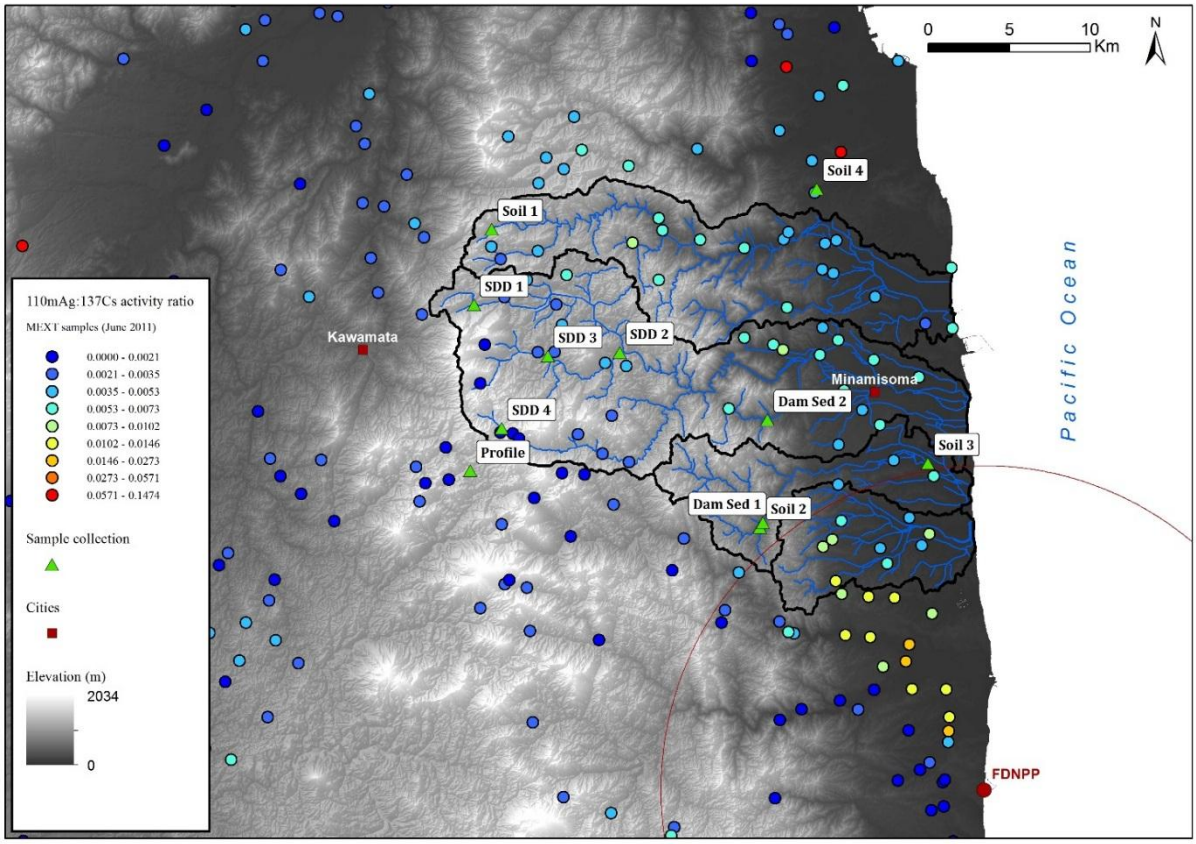


fig4.docx
Click here to download Figure: FIG4.docx

Figure 4.

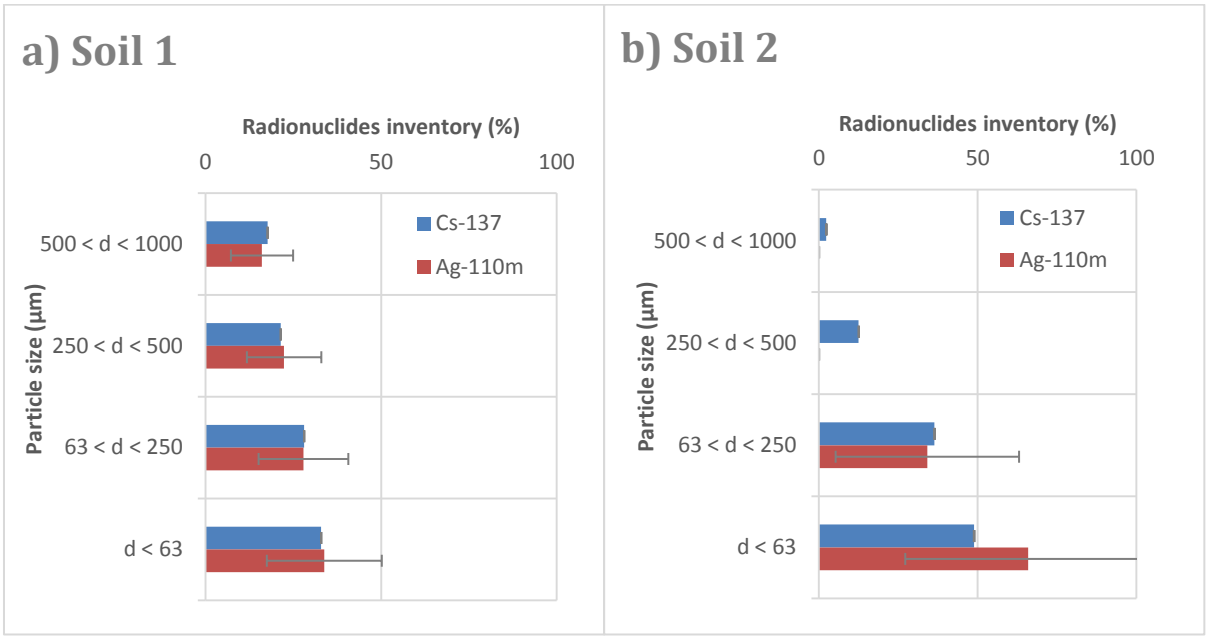


fig5.docx

Click here to download Figure: FIG5.docx

Figure 5.

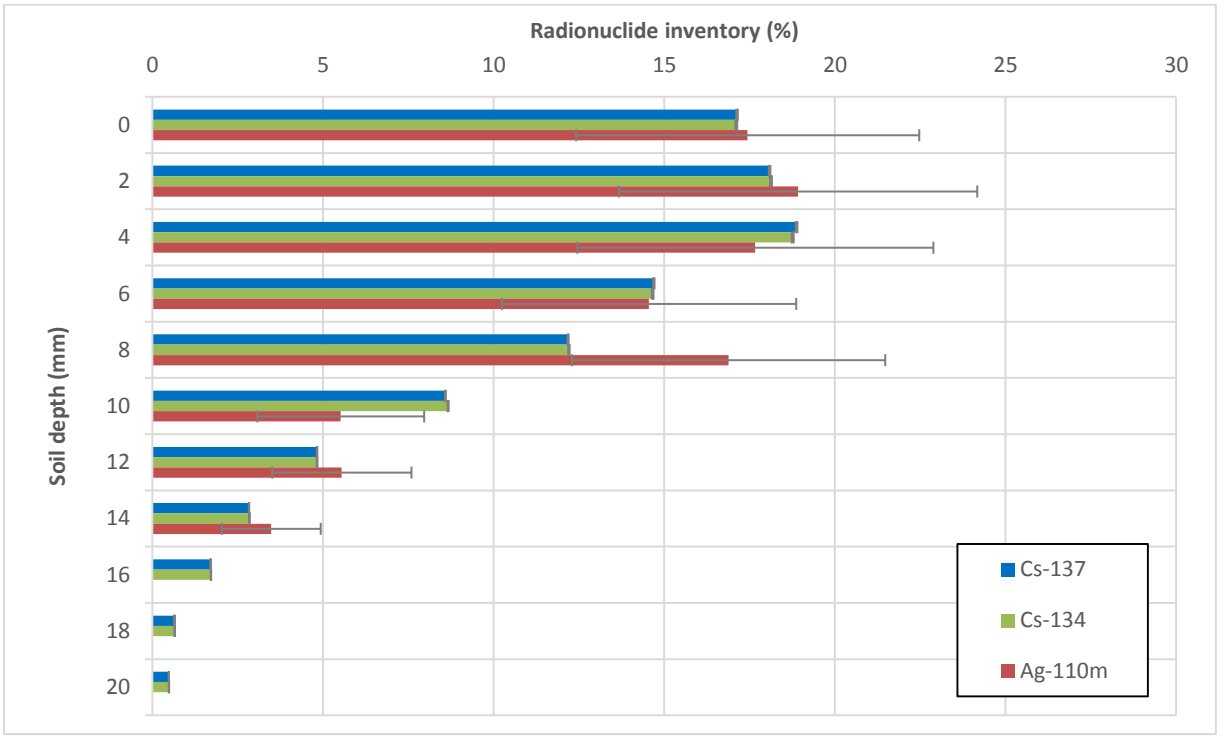


fig6.docx

Click here to download Figure: FIG6.docx

Figure 6.

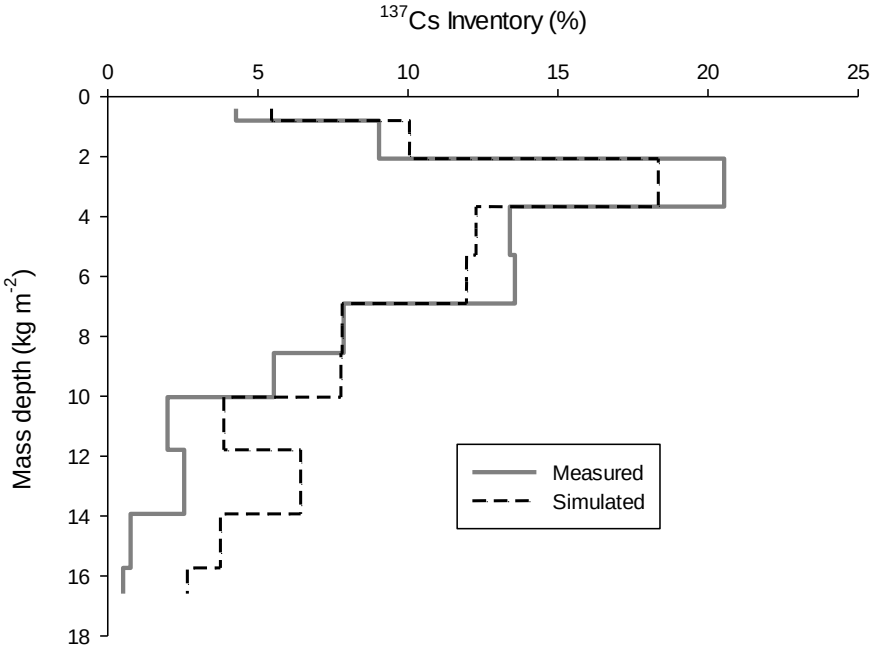


fig7.docx
Click here to download Figure: FIG7.docx

Figure 7.

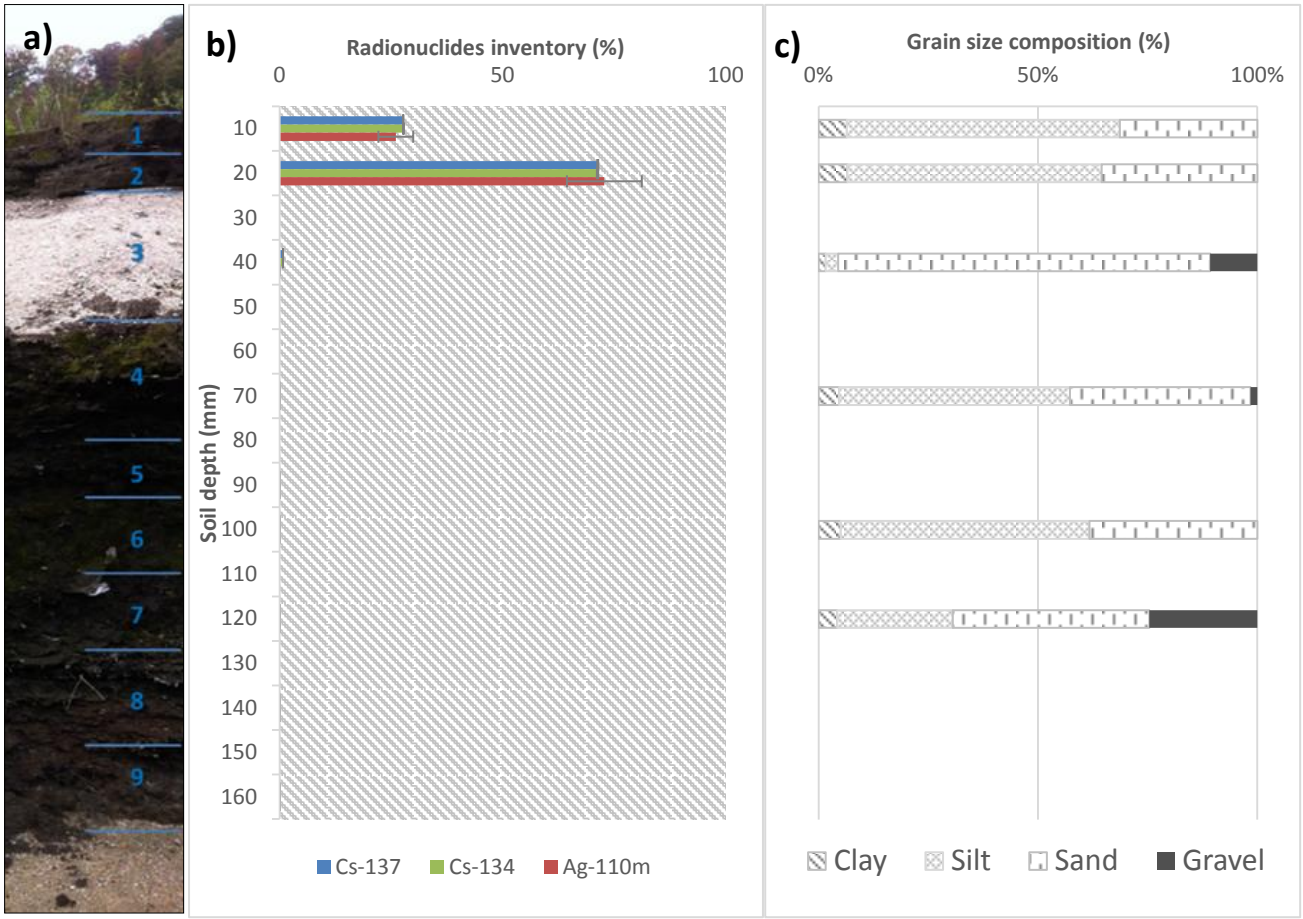


fig8.docx
Click here to download Figure: FIG8.docx

Figure 8.

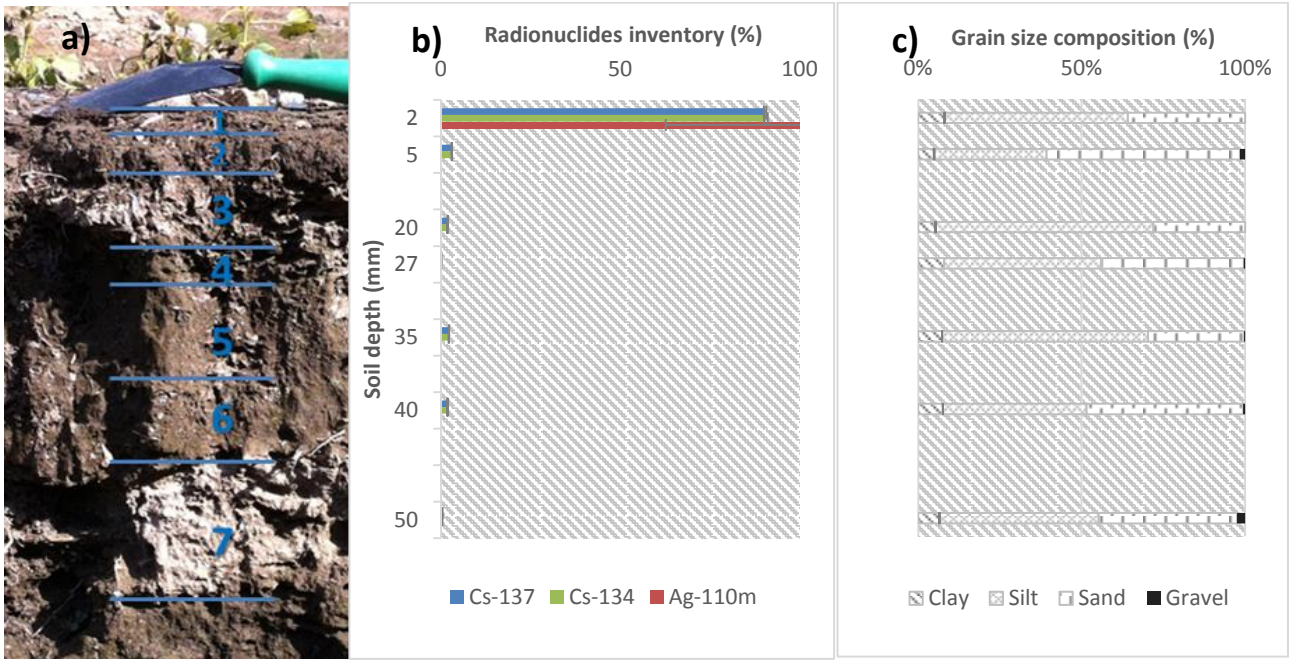


fig9.docx
Click here to download Figure: FIG9.docx

Figure 9.

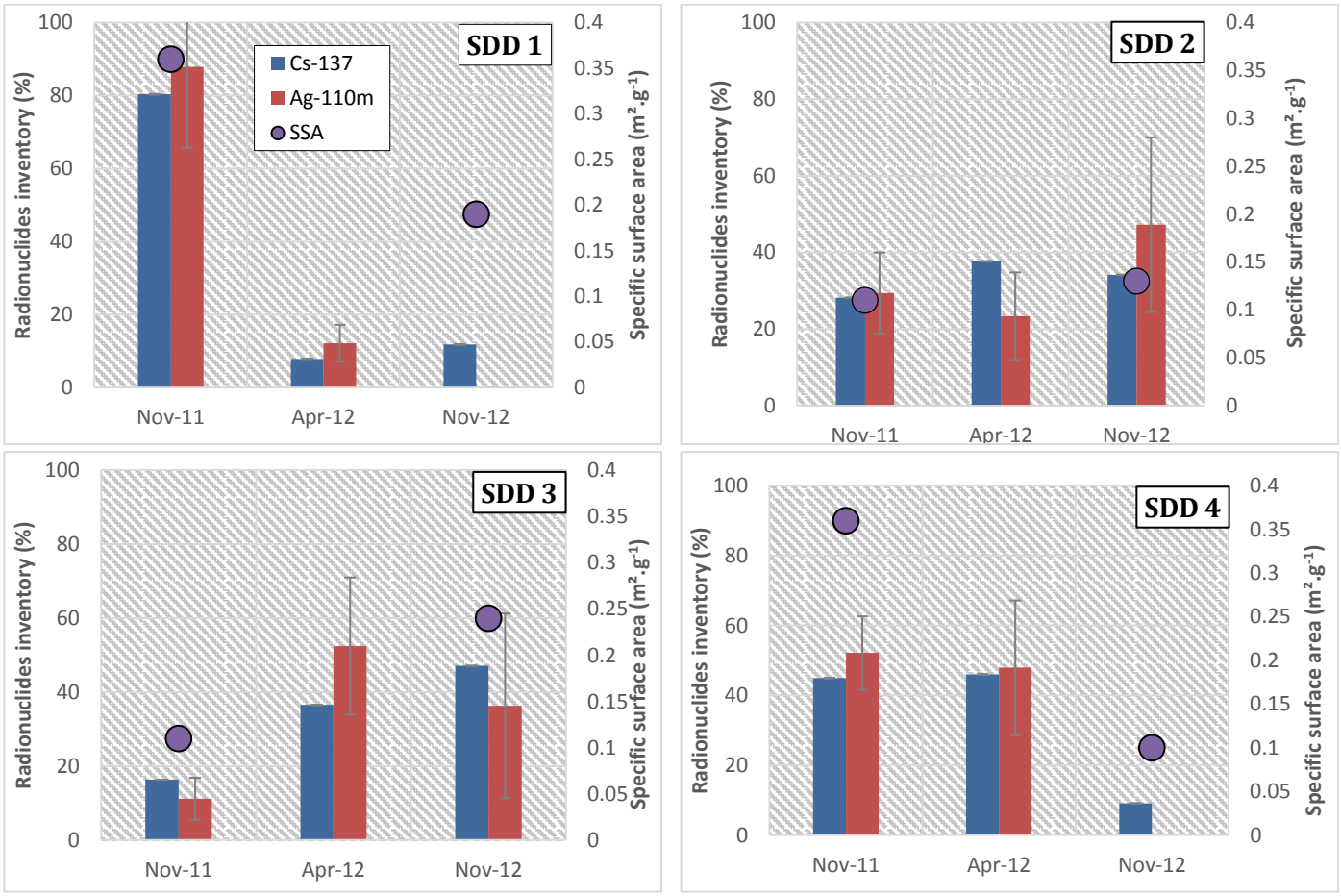


fig10.docx
Click here to download Figure: FIG10.docx

Figure 10

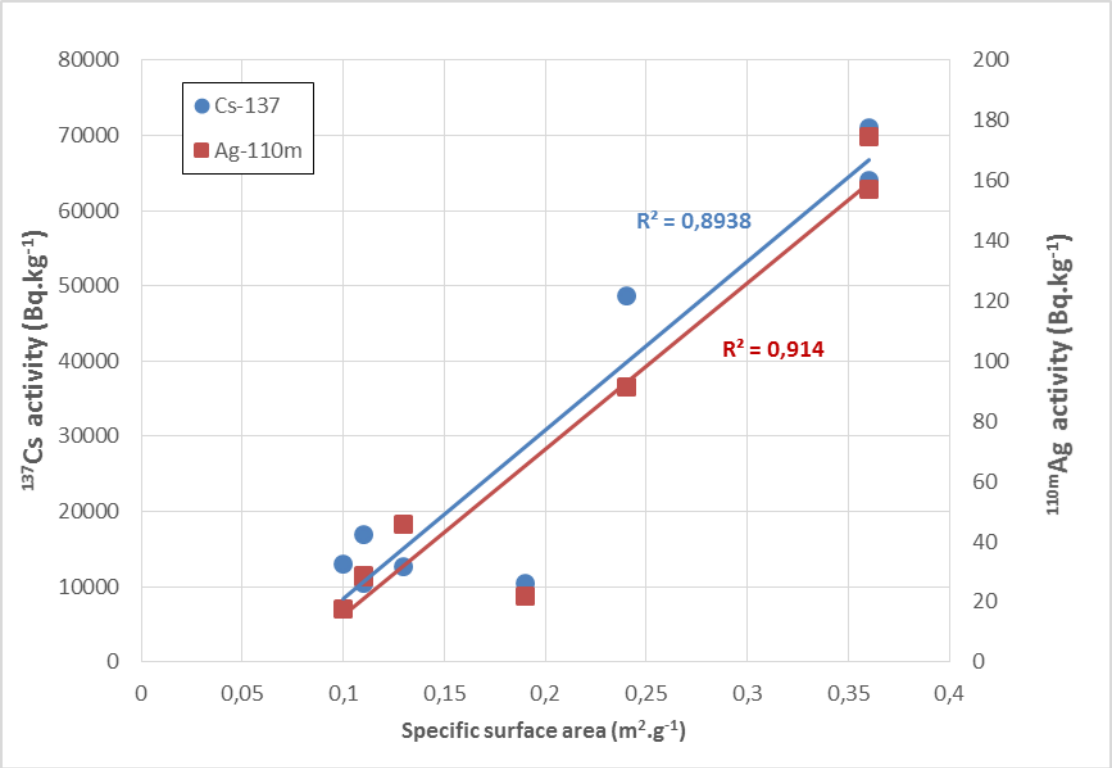


table 1.docx
Click here to download Table: Table 1.docx

Table 1

Literature compilation of radiosilver activities measured in samples collected in the environment in normal and post-accidental conditions.

	Normal conditions				Post-accidental conditions			
	Sample description	Mean (number of samples)	Max	Source	Samples description	Mean (number of samples)	Max	Source
SPM ($Bq.kg_{dry}^{-1}$)	Routine monitoring in France (from 2009 to 2012)	<2 (893)	28	(T.Boissieux, IRSN/LS3E, personal communication)	Not investigated to our knowledge			
	Rhone River, France (from 2005 to 2008)	1 (≈10)	<10	Eyrolle et al. (2012)				
Sediment ($Bq.kg_{dry}^{-1}$)	Routine monitoring in France (from 2009 to 2012) (Bottom sediment)	<1 (279)	<2.75	(T.Boissieux, IRSN/LS3E, personal communication)	In Fukushima Prefecture (14 March 2011) (Sediment drape deposits)	2 – 2390 (162)	2390	Chartin et al. (2013)
Soil ($Bq.kg_{dry}^{-1}$)	Not reported in the literature				In Fukushima Prefecture (11 March 2011)	280 (7)	520	Tazoe et al. (2012)
					In Miyagi Prefecture (26 April 2011)	12 (15)	49	Wanatabe et al. (2012)

SPM : Suspended Particulate Matters

LS3E: Laboratoire de Surveillance de l'Environnement et d'Expertise par Echantillonnage

FDNPP : Fukushima Dai-ichi Nuclear Power Plant

table 2.docx
Click here to download Table: Table 2.docx

Table 2.

Date of collection and location of the samples collected in the framework of this study.

Sample	Date of collection	(WGS 1984): Latitude	Longitude	Experiment
Soil 1	09/11/2012	37.732447	140.688330	1
Soil 2	10/11/2012	37.567039	140.877110	1
Soil 3	10/11/2012	37.602735	140.994663	1
Soil 4	10/11/2012	37.755403	140.916649	1
Profile	04/2012	37.598136	140.673917	2
Dam Sed 1 (Tetsuzen)	10/11/2012	37.569687	140.879102	3
Dam Sed 2 (Takanokura)	08/11/2012	37.626889	140.882307	3
SDD 1	See Table 7	37.690509	140.676251	4
SDD 2	See Table 7	37.664095	140.778413	4
SDD 3	See Table 7	37.662099	140.728151	4
SDD 4	See Table 7	37.621797	140.695852	4

SDD: Sediment Drape Deposit

table 3.docx
Click here to download Table: Table 3.docx

Table 3.

Distribution of radionuclide activities ($Bq.kg^{-1}$) and weight in four grain size fractions of five soils collected across Fukushima radioactive pollution plume. Total activity ($Bq.kg^{-1}$) is also given for the bulk sample.

Sample	500 µm < d < 1000 µm			250 µm < d < 500 µm			63 µm < d < 250 µm			d < 63 µm			Bulk sample activity	
	Weight (%)	^{137}Cs	^{110m}Ag	Weight (%)	^{137}Cs	^{110m}Ag	Weight (%)	^{137}Cs	^{110m}Ag	Weight (%)	^{137}Cs	^{110m}Ag	^{137}Cs	^{110m}Ag
Soil 1	8*	21 166 ± 50**	83 ± 36	16	25 636 ± 56	116 ± 40	42	33 682 ± 64	145 ± 44	32	39 490 ± 90	175 ± 62	n/a	n/a
Soil 2	11	929 ± 14	< 14	14	5009 ± 32	< 26	27	14 600 ± 80	93 ± 64	29	19 608 ± 66	179 ± 54	9912 ± 64	98 ± 52
Soil 3	8	298 ± 8	< 10	14	425 ± 14	< 10	35	446 ± 10	< 12	39	580 ± 16	< 8	506 ± 12	< 12
Soil 4	17	576 ± 12	< 14	12	787 ± 14	< 16	34	665 ± 12	< 14	37	1484 ± 26	27 ± 25	634 ± 26	< 22

d: diameter

n/a: not available

* The remainder of the sample mass correspond to the gravel fraction (>1000 µm)

** Uncertainties on results were estimated by combining counting statistics and calibration uncertainties. Summing and self-absorption effects were taken into account by analysing standards with similar densities and characteristics as the collected samples.

table 4.docx
Click here to download Table: Table 4.docx

Table 4.

Depth distribution of ^{137}Cs and ^{110m}Ag concentrations in the soil profile.

Depth (mm)	^{137}Cs (Bq.kg^{-1})	^{110m}Ag (Bq.kg^{-1})	Dry bulk density (g.cm^{-3})	Mass depth (kg.m^{-2})
0 – 2	44 698 ± 74	100 ± 34	0.19	0.4
2 – 4	47 189 ± 72	109 ± 34	0.40	1.2
4 – 6	49 254 ± 76	101 ± 38	0.87	2.9
6 – 8	38 335 ± 64	84 ± 32	0.73	4.4
8 – 10	31 776 ± 58	97 ± 28	0.89	6.2
10 – 12	22 393 ± 54	32 ± 24	0.73	7.6
12 – 14	12 575 ± 38	32 ± 18	0.92	9.5
14 – 16	7374 ± 28	20 ± 14	0.56	10.6
16 – 18	4439 ± 22	< 12	1.19	13.0
18 – 20	1674 ± 14	< 16	0.94	14.9
20 - 22	1241 ± 22	< 16	0.86	16.6

table 5.docx
Click here to download Table: Table 5.docx

Table 5.

Depth, radionuclide activities and grain size proportions of the sequence of sediment accumulated behind Tetsuzen Dam (Ota River)

	Radionuclide activities and activity ratio			Grain size proportions			
Depth (cm)	^{137}Cs (Bq.kg^{-1})	^{110m}Ag (Bq.kg^{-1})	^{110m}Ag:^{137}Cs	Clay (%)	Silt (%)	Sand (%)	Gravel (%)
0 - 10	64 195 ± 210	649 ± 142	0.010 ± 0.002	6	62	31	0
10 - 20	165 217 ± 280	1813 ± 196	0.011 ± 0.001	7	58	35	0
20 - 40	1790 ± 24	< 20	n/a	2	3	85	11
40 - 70	146 ± 8	< 18	n/a	5	53	41	2
70 - 85	68 ± 8	<22	n/a	n/a	n/a	n/a	n/a
85 - 100	33 ± 8	< 40	n/a	5	57	38	0
100 - 110	147 ± 20	< 68	n/a	4	26	45	25
110 – 140	26 ± 4	< 14	n/a	n/a	n/a	n/a	n/a
140 – 162	77 ± 10	< 18	n/a	n/a	n/a	n/a	n/a

n/a: not available

table 6.docx
Click here to download Table: Table 6.docx

Table 6.

Depth, radionuclide activities and grain size proportions of the sequence of sediment accumulated behind Takanokura Dam (Nitta River).

	Radionuclide activities ($Bq.kg^{-1}$)		Activity ratio	Grain size proportions			
Depth (cm)	^{137}Cs	^{110m}Ag	^{110m}Ag:^{137}Cs	Clay (%)	Silt (%)	Sand (%)	Gravel (%)
0 - 2	28 744 ± 120	246 ± 88	0.0085 ± 0.0030	8	56	36	0
2 - 5	967 ± 30	< 32	n/a	5	34	59	2
5 - 20	616 ± 18	< 18	n/a	5	67	28	0
20 - 27	28 ± 4	< 12	n/a	8	48	44	0
27 - 35	728 ± 16	< 18	n/a	7	63	29	0
35 - 40	592 ± 10	< 12	n/a	8	44	48	1
40 - 50	124 ± 6	< 16	n/a	7	49	42	2

n/a: not available

table 7.docx
Click here to download Table: Table 7.docx

Table 7.

Characteristics of the riverbed sediment from the upper part of the Nitta River catchment collected at the same locations during the three fieldwork campaigns.

Sample	Sampling date	^{137}Cs activity (Bq.kg^{-1})	^{110m}Ag activity (Bq.kg^{-1})	^{110m}Ag:^{137}Cs	SSA (m².g^{-1})	pH
SDD 1	Nov-2011	71 014 ± 108	157 ± 30	0.0022 ± 0.0004	0.36	n/a
	Apr-2012	6 939 ± 34	22 ± 16	0.0031 ± 0.0023	n/a	n/a
	Nov-2012	10 394 ± 62	< 38	n/a	0.19	6 ± 0.5
SDD 2	Nov-2011	10 385 ± 32	29 ± 10	0.0028 ± 0.0010	0.11	n/a
	Apr-2012	13 885 ± 34	23 ± 18	0.0016 ± 0.0013	n/a	n/a
	Nov-2012	12 583 ± 48	46 ± 34	0.0036 ± 0.0027	0.13	6 ± 0.5
SDD 3	Nov-2011	16 898 ± 66	29 ± 22	0.0017 ± 0.0013	0.11	n/a
	Apr-2012	337 786 ± 72	132 ± 34	0.0035 ± 0.0009	n/a	n/a
	Nov-2012	48 680 ± 178	92 ± 55	0.0019 ± 0.0011	0.24	5.5 ± 0.5
SDD 4	Nov-2011	64 093 ± 100	175 ± 16	0.0027 ± 0.0002	0.36	n/a
	Apr-2012	65 599 ± 106	161 ± 24	0.0024 ± 0.0004	n/a	n/a
	Nov-2012	12 949 ± 74	< 44	n/a	0.1	6

n/a: not available

table 8.docx
Click here to download Table: Table 8.docx

Table 8

Comparison of ^{110m}Ag:^{137}Cs activity ratio between soil and sediment drape deposits collected during the three campaigns in the upper part of the Nitta River catchment. All values were decay-corrected to 14 march 2011.

^{110m}Ag:^{137}Cs activity ratio	Soil (based on MEXT data)	SDD
Nov-11	0.0023 ± 0.008	0.0023 ± 0.0005
Apr-12		0.0027 ± 0.0008
Nov-12		0.0022 ± 0.0010

SDD: Sediment Drape Deposits